Discovery of Novel Glycerolated Quinazolinones from *Streptomyces* sp. MBT27

Nataliia Machushynets [1], Changsheng Wu [1,2,] *, Somayah S. Elsayed [1], Thomas Hankemeier [3] and Gilles P. van Wezel [1,] *

[1] *Molecular Biotechnology, Institute of Biology, Leiden University, Sylviusweg 72, 2333 BE, The Netherlands*

[2] *State Key Laboratory of Microbial Technology, Institute of Microbial Technology, Shandong University, Qingdao 266237, P.R. China*

[3] *Leiden Academic Centre for Drug Research (LACDR), Leiden University, Einsteinweg 55, 2333 CC, Leiden, The Netherlands*

* Author for correspondence. Tel: +31 71 5274310; email: g.wezel@biology.leidenuniv.nl, or wcs0313@gmail.com

Abstract

Actinobacteria are a major source of novel bioactive natural products. A challenge in the screening of these microorganisms lies in finding the favorable growth conditions for secondary metabolite production and dereplication of known molecules. Here, we report that *Streptomyces* sp. MBT27 produces 4-quinazolinone alkaloids in response to elevated levels of glycerol, whereby quinazolinones A (**1**) and B (**2**) form a new sub-class of this interesting family of natural products. Global Natural Product Social molecular networking (GNPS) resulted in a quinazolinone-related network that included anthranilic acid (**3**), anthranilamide (**4**), 4(3H)-quinazolinone (**5**) and 2,2-dimethyl-1,2-dihydroquinazolin-4(3*H*)-one (**6**). Actinomycins D (**7**) and X2 (**8**) were also identified in the extracts of *Streptomyces* sp. MBT27. The induction of quinazolinone production by glycerol combined with biosynthetic insights provide evidence that glycerol is integrated into the chemical scaffold. The unprecedented 1,4-dioxepane ring that is spiro-fused into the quinazolinone backbone, is most likely formed by intermolecular etherification of two units of glycerol. Our work underlines the importance of varying the growth conditions for the discovery of novel natural products and for understanding their biosynthesis.

Keywords: 4(3*H*)-quinazolinones, molecular networking, metabolomics, carbon source

39 **Introduction**

40 Actinobacteria are a major source of bioactive compounds, producing some two third of all antibiotics
41 as well as molecules with a wide variety of activities such as anticancer, antifungal and
42 immunosuppressant [2,4]. Traditionally, microbial natural product (NP) discovery has been done via
43 high-throughput screening followed by iterative bioassay-guided fractionation and structure
44 elucidation. While such pipelines were extremely successful and delivered a plethora of therapeutic
45 agents, in the modern era the large pharmaceutical companies move out of NP-discovery programs
46 due to high cost and chemical redundancy [1,9,28]. At the same time, the power of genome sequencing
47 brought the recognition that microorganisms harbor a vast and yet untapped biosynthetic potential,
48 and it rapidly became clear that the potential for metabolic diversity of even the best-studied model
49 organisms as producers of natural products had been grossly underestimated [3,11,18]. How could
50 these compounds have been missed by the very extensive HT screening campaigns of the 20th
51 century? The answer is that many of the biosynthetic gene clusters (BGCs) discovered by genome
52 mining are poorly expressed or cryptic under laboratory conditions [21,27]. A drug-discovery pipeline
53 that is rapidly gaining momentum involves combining genome mining with fluctuating the culturing
54 conditions to achieve differential synthesis of NPs, followed by the metabolic profiling-based
55 identification of the bioactivity of interest [13,46]. A major challenge thereby lies in finding the
56 appropriate chemical triggers or ecological cues to elicit the production of cryptic antibiotics (recently
57 reviewed in [33,48,49]). The use of chemical elicitors is thereby a promising approach [10,49].

58 Manipulation of fermentation conditions for promising producer strains, known as the "one
59 strain many compounds" (OSMAC) approach, is an effective way of enhancing the production of
60 secondary metabolites [32,5]. The regulatory networks that control the production of bacterial natural
61 products respond strongly to changes in carbon, nitrogen or phosphate concentration [40,39]. The re-
62 isolation of known metabolites is a major bottleneck in the discovery of new bioactive natural products.
63 A crucial step in this regard is the early identification of already known substances, in order to
64 concentrate the efforts on the discovery of new ones, a process known as dereplication [15]. Current

65 dereplication strategies include hyphenated techniques, such as LC-MS, LC-NMR, LC-NMR-MS, and LC-
66 SPE-NMR. Bioactivity fingerprinting has also been used to dereplicate natural products based on their
67 biological modes of action [35], while molecular networking is a powerful tool for the visualization and
68 dereplication of natural products [47,44]. Mass spectrometry-based molecular networking relies on
69 clustering of molecules based on similarities in their MS/MS fragmentation patterns, which depends
70 on the structural features of the ionized molecules. The resulting clusters allow scientists to visually
71 explore the metabolites produced by a given strain under a specific growth condition, allowing rapid
72 dereplication of known compounds by automated spectral library searches, and to visualize their
73 unknown structural analogues [43].

74 In this work we analyzed the potential of *Streptomyces* sp. MBT27 as producer of natural
75 products in response to changes in the carbon source. The strain had previously been identified as a
76 promising producer of NPs [50]. Extensive fluctuations in the secondary metabolite profiles were
77 observed depending on the carbon source used, and statistical methods combined with GNPS
78 molecular networking identified a family of known as well as novel quinazolinone compounds, in
79 response to high concentrations of glycerol. Quinazolinones are heterocyclic compounds with a wide
80 range of medical applications, such as antimicrobial, antiviral, antituberculosis and as enzyme
81 inhibitors (reviewed in [23,16,19]). Combination of MS and NMR methods identified the novel
82 quinazolinones A (**1**) and B (**2**), which further expands the chemical space of this rich family of natural
83 products.

84

85 **Materials and Methods**

86 **Bacterial strain, growth conditions**

87 *Streptomyces* sp. MBT27 was obtained from the Leiden University strain collection and had previously
88 been isolated from the Qingling Mountains, Shanxi province, China [50]. Cultures were grown in
89 triplicate in 100 mL Erlenmeyer flasks with 30 mL of liquid minimal medium (MM; [20]), supplemented
90 with various carbon sources, and inoculated with 10 µL of 10^9/mL spore suspension. The carbon

91 sources (percentages in w/v) were: 1% mannitol + 1% glycerol, 1% mannitol, 2% mannitol, 1% glycerol,
92 2% glycerol, 1% glucose, 2% glucose, 1% fructose, 1% arabinose or 1% *N*-acetylglucosamine (GlcNAc).
93 The cultures were incubated in a rotary shaker at 30 °C at 220 rpm for seven days.
94
95 **General Experimental Procedures**
96 NMR spectra were recorded in deuterated methanol (CD_3OD) on a Bruker 600 MHz, and were
97 referenced using the residual ^1H signal of deuterated solvent at 3.30 ppm. FT-IR was measured on
98 Perkin-Elmer FT-IR Spectrometer Paragon 1000. UV measurements were performed using a Shimadzu
99 UV mini-1240. Optical rotations were measured on a JASCO P-1010 polarimeter. HPLC purification was
100 performed on Waters preparative HPLC system comprised of 1525 pump, 2707 autosampler, 2998 PDA
101 detector, and Water fraction collector III. The columns used were SunFire C_{18} column (5 µm, 100 Å, 10
102 × 250 mm) and SunFire C_{18} column (10 µm, 100 Å, 19 × 150 mm). TLC was performed using aluminum
103 plates coated with silica gel 60 F_{254} (Merck). All organic solvents and chemicals were of analytical
104 or LCMS grade, depending on the experiment.
105
106 **Metabolite profiling**
107 Following fermentation, culture supernatants were extracted with ethyl acetate (EtOAc) and
108 evaporated under reduced pressure. For LC-ESI-QTOFMS analyses, extracts were dissolved in MeOH
109 to a final concentration of 1 mg/mL, and 1 µL was injected into Waters Acquity UPLC system equipped
110 with Waters Acquity HSS C_{18} column (1.8 µm, 100 Å, 2.1 × 100 mm), which is coupled to Agilent 6530
111 QTOF MS equipped with Agilent Jet Stream ESI source (Agilent Technologies, Inc., Palo Alto, CA, USA).
112 For the LC, solvent A was 95% H_2O, 5% acetonitrile (ACN) and 0.1% formic acid; solvent B was 100%
113 ACN and 0.1% formic acid. The gradient used was 2% B for 1 min, 2–85% for 9 min, 85–100% for 1 min,
114 and 100% for 3 min. The flow rate used was 0.5 mL/min. As for the MS, the following ESI source
115 parameters were used: capillary voltage 3 kV, source temperature 325 °C, drying gas flow rate 10
116 L/min, and fragmentor 175 V. Full MS spectra were acquired in positive mode in the range of 100-

117 1700 *m/z*, in the extended dynamic range mode. Internal reference masses of purine and Agilent HP-
118 921 were continuously delivered to the ESI source through an Agilent 1260 isocratic pump.
119 Thermo Instruments MS system (LTQ Orbitrap XL, Bremen, Germany) equipped with an
120 electrospray ionization source (ESI) was used for LC-MS/MS analysis. The Waters Acquity UPLC system
121 equipped with Waters Acquity PDA was run using a SunFire Waters C_{18} column (3.5 µm, 100 Å, 4.6 ×
122 150 mm), at a flow rate of 0.9 mL/min. Solvent A was 95% H_2O, 5% acetonitrile (ACN) and 0.1% formic
123 acid; solvent B was 100% ACN and 0.1% formic acid. The gradient used was 2% B for 1 min, 2-85% for
124 15 min, 85–100% for 3 min, and 100% for 3 min. As for the MS, the following ESI parameters were
125 used: capillary voltage 5 V, spray voltage 3.5 kV, capillary temperature 300 °C, auxiliary gas flow rate
126 10 arbitrary units, and sheath gas flow rate 50 arbitrary units. Full MS spectra were acquired in the
127 Orbitrap in positive mode at a mass range of 100–2000 *m/z*, and FT resolution of 30000. Data
128 dependent MS^2 spectra were acquired in the ion trap for the three most intense ions using collision
129 induced dissociation (CID). The resulting chemical data were compared with those in SciFinder and
130 Antibase [24].
131
132 **Up-scale fermentation and isolation of metabolites (1) and (2)**
133 For up-scale fermentation, *Streptomyces* sp. MBT27 was grown in eight 2000 mL Erlenmeyer flasks,
134 each containing 500 mL liquid MM supplemented with 2% w/v glycerol at 30 °C for seven days. The
135 metabolites were extracted from the culture broth using EtOAc, then the solvent was evaporated
136 under reduced pressure at 40 ºC. The crude extract (1.4 g) was adsorbed onto 1.4 g silica gel (pore
137 size 60 Å, 70-230 mesh, Sigma Aldrich), and loaded on silica column, which was eluted using gradient
138 mixtures of *n*-hexane, acetone, and MeOH. The fractions eluted with acetone 100% were combined,
139 reconstituted in MeOH, and injected into the preparative SunFire column (19 x 150 mm), which was
140 eluted with H_2O:MeOH gradient of 7–100% in 30 min, at a flow rate of 15 mL/min, to yield five
141 fractions. Quinazolinones A and B were further purified on the semi-preparative SunFire column (10 x
142 250 mm), run at 3 mL/min. Fraction 2 was eluted using H_2O:MeOH gradient of 20–40% in 20 min, to

143 yield Quinazolinone A (**1**, 1 mg). On the other hand, Fraction 3 was eluted using H_2O:MeOH gradient
144 of 30-40% in 20 min, to yield Quinazolinone B (**2**, 1.5 mg).
145 ***Quinazolinone A (1)***: colorless, amorphous powder; $[\alpha]_D^{20}$ 2.3 (c 0.1, MeOH); UV (MeOH) λ_{max} (log ε)
146 224 (4.09), 322 (2.98) nm; IR ν_{max} 3334, 2922, 1652, 1475, 1052 cm^{-1}; ^1H and ^{13}C NMR data, see Table
147 1; HRESIMS (positive mode) *m/z* 281.1130 $[M + H]^+$ (calcd. for $C_{13}H_{17}N_2O_5$, 281.1132).
148 ***Quinazolinone B (2)***: colorless, amorphous powder, UV (MeOH) λ_{max} (log ε) 226 (4.18), 347 (3.03) nm;
149 IR ν_{max} 3350, 2950, 1649, 1526, 1049, 751 cm^{-1}; ^1H and ^{13}C NMR data, see Table 1; HRESIMS (positive
150 mode) *m/z* 209.0915 $[M + H]^+$ (calcd. for $C_{10}H_{13}N_2O_3$, 209.0921).
151
152 **Computation of mass spectral networks**
153 MS/MS raw data were converted to a 32 bit mzXML file using MSConvert (ProteoWizard) [6] and
154 spectral networks were assembled using Global Natural Product Social molecular networking (GNPS)
155 (https://gnps.ucsd.edu) as described [43]. For both parent and MS/MS fragment ions, the mass
156 tolerance was set to 0.5 Da, while the minimum cosine score was set to 0.7. The data were clustered
157 using MSCluster with a minimum cluster size of three spectra. The spectra in the network were also
158 searched against GNPS spectral libraries. A minimum score of 0.5 was set for spectral library search,
159 with at least two fragment peaks matching. Cytoscape 3.5.1. was used for visualization of the
160 generated molecular networks [37]. The edge thickness was set to represent the cosine score, with
161 thicker lines indicating higher similarity between nodes. LC-MS/MS data were deposited in the
162 MassIVE Public GNPS data set (MSV000082988). The molecular networking job in GNPS can be found
163 at https://gnps.ucsd.edu/ProteoSAFe/status.jsp?task=8fd1fcfa0ff744a9808e80bc7be12115. The
164 annotated MS/MS spectra were deposited in the GNPS spectral library for quinazolinone A
165 (CCMSLIB00004684355), and B (CCMSLIB00004684354).
166
167 **Statistical analysis**

168 Prior to statistical analysis, mzXML files were imported into Mzmine 2.31 [29] for data processing. Mass
169 ion peaks were detected using the exact mass algorithm with a noise level set to 1.0×10^4. Afterwards,
170 chromatograms were built for the detected masses with a minimum time span of 0.05 min, *m/z*
171 tolerance of 0.001 *m/z* and minimum height of 1.0×10^4. Chromatogram deconvolution was then
172 performed using local minimum search algorithm (search minimum in RT range 0.1 min,
173 chromatographic threshold 90%, minimum relative height 1%, minimum absolute height 1.0×10^4,
174 minimum ratio of peak top/edge 2 and peak duration range 0.05–3 min). In the generated peak lists,
175 isotopes were identified using isotopic peaks grouper (*m/z* tolerance 0.001 *m/z* and retention time
176 tolerance 0.1 min), and variations in retention time were reduced using retention time normalizer (*m/z*
177 tolerance 0.001 *m/z* and retention time tolerance 1 min). All the peak lists were subsequently aligned
178 using join aligner (*m/z* tolerance 0.001 *m/z*, *m/z* weight 20, retention time tolerance 0.1 min, and
179 retention time weight 20), and missing peaks were detected through gap filling using peak finder
180 (intensity tolerance 1.0%, *m/z* tolerance 0.001 *m/z*, and retention time tolerance of 0.2 min). Finally,
181 the aligned peak list was exported as a comma separated file for statistical analysis.

182 Statistical analysis was performed using MetaboAnalyst [7], where log transformation and
183 pareto scaling was initially applied to the data. A heat map of all detected masses, among the different
184 growth conditions, was generated in MetaboAnalyst, to which additional hierarchical clustering
185 analysis (HCA) was performed using Euclidean distance measure and Ward clustering algorithm.
186 Student's *t*-tests with multiple testing correction (Benjamini Hochberg false discovery rate or FDR)
187 were used to determine significant differences in the intensities of the metabolites, under two
188 different growth conditions. The thresholds set for statistically significant differences were a fold
189 change ≥ 4, together with FDR corrected *p*-value ≤ 0.05 Based on these criteria, a volcano plot was
190 generated. To identify the difference in intensity of a single mass feature among multiple growth
191 conditions, one-way ANOVA was performed, followed by a *post hoc* Tukey's honest significant
192 difference (HSD) test.

193

194 **RESULTS AND DISCUSSION**

195

196 **The influence of carbon sources on secondary metabolite production**

197 Previous screening of our in-house actinomycete collection, obtained from remote mountain soils,
198 showed it is a promising source of new bioactive compounds [50]. Under specific growth conditions,
199 these isolates exert potent inhibitory activity against the so-called ESKAPE pathogens [30]
200 *Enterococcus faecium*, *Staphylococcus aureus*, *Klebsiella pneumoniae*, *Acinetobacter baumannii*,
201 *Pseudomonas aeruginosa* and *Enterobacter* spp. In the current study, the potential of one of the
202 *Streptomyces* strains in our collection, namely *Streptomyces* sp. MBT27, was analyzed to study the
203 effect of carbon sources on its metabolite profile. Traditional approaches such as changes in
204 fermentation conditions, are known to induce significant changes in the microbial metabolome.
205 Culture medium components, and particularly the carbon source, have major effects on the production
206 of secondary metabolites [41,34,5,25]. The differential production of small molecules is ideal for
207 metabolomics studies, whereby metabolic variations are correlated statistically to bioactivity, thus
208 facilitating the identification of the bioactive molecule of interest [46,49]. To establish the potential of
209 *Streptomyces* sp. MBT27, the strain was grown in liquid minimal media containing different carbon
210 sources, namely (percentages in w/v): 1% of both mannitol and glycerol, 1% mannitol, 2% mannitol,
211 1% glycerol, 2% glycerol, 1% glucose, 2% glucose, 1% fructose, 1% arabinose, or 1% *N*-
212 acetylglucosamine (GlcNAc). The latter is an elicitor of antibiotic produciton, via metabolic interference
213 with the global nutrient sensory network controlled by DasR [38,31]. Phosphate buffer was omitted
214 from the MM as it repressed the production of secondary metabolites by *Streptomyces* sp. MBT27
215 (data not shown). To identify the secondary metabolites in the cultures, supernatants were extracted
216 with EtOAc, and the resulting crude extracts subjected to LC-MS analysis. Using the LC-MS data, a heat
217 map with added hierarchical clustering was generated, to visualize the production of different
218 metabolites under different culture conditions (Fig. 1). Hierarchical clustering analysis of the LC-MS
219 data allows effective comparative analysis of metabolomics data, and the heat map revealed major

220 differences in the metabolic profiles of *Streptomyces* sp. MBT27, whereby different groups of
221 metabolites were enhanced depending on the carbon source used. Interestingly, not only the type of
222 carbon source, but especially also the concentration resulted in large changes in the metabolic profiles.
223 Doubling the concentration of either glycerol or glucose from 1% to 2% had a particularly profound
224 change on the metabolic profile. Thin layer chromatography (TLC) was conducted to compare
225 metabolic profiles of the 1% and 2% glycerol-grown cultures. Interestingly, this revealed that several
226 fluorescent compounds were differentially produced in the extracts of 2% glycerol-grown cultures
227 relative to those produced in 1% glycerol (Fig. 2a). In order to provide statistical relevance to the data,
228 the metabolic profiles of 1% and 2% glycerol-grown cultures were compared using a volcano plot (Fig.
229 2b). The volcano plot was then searched for the mass features which increased in production in 2%
230 glycerol as compared to 1%. A mass of *m/z* 281.1151 (**1**) stood out as its intensity had increased by
231 around 7000 fold (*p*-value = 0.002) in cultures fermented in 2% glycerol as compared to 1%.

232 Global Natural Product Social (GNPS) molecular networking [43] was employed to detect the
233 MS/MS structural relatedness among molecules in an automated manner; the software generates a
234 molecular network wherein molecules with related scaffolds cluster together [43]. A network
235 representing the ions detected in the crude extract of *Streptomyces sp.* MBT27 grown with 2% glycerol
236 was constructed, revealing 183 nodes clustered in 19 spectral families (Fig. 3). GNPS dereplication
237 based on matching with its MS/MS spectral database highlighted some known metabolites. These
238 included anthranilic acid (**3**), anthranilamide (**4**) [36], actinomycin D (**7**), and actinomycin X2 (**8**) [42].
239 The annotation of the compounds was supported by comparison of the exact mass, fragmentation
240 pattern, and UV spectra, with reference data. Moreover, crude extracts of MBT27 possessed
241 antimicrobial activity against *B. subtilis*, which was most likely due to the expression of actinomycins
242 (data not shown). Additional metabolites could be dereplicated through manual comparison of their
243 spectral data against the microbial natural products database Antibase. These previously described
244 metabolites were 4(3*H*)-quinazolinone (**5**) [22] and 2,2-dimethyl-1,2-dihydroquinazolin-4(3*H*)-one (**6**)
245 [8].

246 Besides known molecules, the network also contained many mass features that could not be
247 assigned to any of the previously identified metabolites. One of these was an ion with an *m/z* value of
248 281.1151 (**1**), which was very highly increased in intensity (7000 fold, *p*-value = 0.002) when the
249 glycerol concentration was increased from 1% to 2%. It was closely connected (cosine score 0.91) to
250 another upregulated ion with an *m/z* value of 209.0932 (**2**), which was also not previously reported.
251 Both ions were part of the large spectral family comprising the annotated anthranilic acid (**3**),
252 anthranilamide (**4**), and the 4-quinazolinones **5** and **6**, suggesting that they are structurally related
253 metabolites. The relationship between the increase in glycerol concentration and the strong increase
254 in the production of the compounds **1** and **2**, was investigated further by expanding the range of
255 glycerol concentrations and analyzing the metabolic profiles. For this, *Streptomyces* sp. MBT27 was
256 cultured in glycerol concentrations ranging from 1-4% (w/v). ANOVA, followed by a *post hoc* Tukey's
257 HSD test, was performed to trace the variation in the production of **1** and **2** among the different
258 culturing conditions. A box plot was used to visualize such variation (Fig. S1). As observed earlier, the
259 production of **1** and **2** was significantly increased when the glycerol concentration was increased from
260 1% to 2%. However, further increase in glycerol concentration (3% and 4%), did not lead to any
261 significant increase in the production of **1** and **2**. Accordingly, MM with 2% glycerol was used to culture
262 the bacteria, for the purpose of purification and identification of the new metabolites **1** and **2**.
263
264 **Isolation and structure elucidation of novel quinazolinones**
265 To elucidate the structure of **1** and **2**, upscale fermentation was done to obtain larger quantities of the
266 compounds. For this, *Streptomyces* sp. MBT27 was fermented in a total of 4 L of liquid MM
267 supplemented with 2% glycerol, and the supernatant was extracted with EtOAc. Following repeated
268 chromatographic isolation, compounds **1** and **2** were obtained as pure, colorless, amorphous powders.
269 Both compounds were fluorescent, showing UV absorption maxima at 224 and 322 nm and at 226 and
270 347 nm, respectively. The final structures of **1** and **2** were determined by the combination of NMR and
271 high resolution MS (Fig. 4).

272 The high resolution mass of *m/z* 281.1151 for an $[M + H]^+$ established a molecular formula of
273 $C_{13}H_{16}N_2O_5$, with seven degrees of unsaturation, for **1** (yield 0.25 mg/L). The deduced molecular
274 formula was corroborated by the ^{13}C NMR attached proton test (APT) spectrum that exhibited 13
275 carbons in total. On the other hand, the ^1H NMR spectrum of **1** (Table 1) presented four coupling
276 aromatic signals at δ_H 7.88 (dd, *J* = 7.8, 1.2, H-5), 7.07 (t, *J* = 7.8, H-6), 7.46 (td, *J* = 7.8, 1.2, H-7), and
277 7.23 (brd, *J* = 7.8, H-8), indicating an *o*-disubstituted aromatic benzene system. The HMBC correlation
278 (Fig. 5) from H-5 to C-4 (δ_C 166.1) confirmed one of substituents on the benzene ring to be an
279 ester/amide carbonyl group, while the downfield chemical shift of C-8a at δ_C 143.7 indicated it was
280 nitrogenated. Four O-bearing methylene groups at δ_H 4.43 (d, *J* = 9.0, H-1'a) and 4.24 (d, *J* = 9.0, H-1'b);
281 3.59 (d, *J* = 11.4, H-2'a) and 3.47 (d, *J* = 11.4, H-2'b); 3.86 (d, *J* = 12.6, H-1''a) and 3.80 (d, *J* = 12.6, H-
282 1''b); and 3.66 (d, *J* = 3.0, H_2-3'') were resolved by HSQC experiments. Three of these methylene groups
283 were part of a 1,4-dioxepane ring system, which was established based on the HMBC correlations
284 observed from H-1' to C-2 (δ_C 79.0) and C-2' (δ_C 64.6), from H-2' to C-1'' (δ_C 65.7), and from H-1' to the
285 hemiacetal C-2'' (δ_C 102.9). The remaining oxymethylene group CH_2-3'' was connected to C-2'' based
286 on the HMBC correlations observed from H_2-3'' to C-1'' and C-2''. The two substructures obtained
287 accounted for all of the oxygens and six out of the seven degrees of unsaturation required by the
288 molecular formula of **1**. Accordingly, an additional ring including two nitrogen atoms was deduced to
289 connect the two substructures, forming a 4-quinazolinone ring. Consequently, compound **1** was
290 identified to be a *di*-glycerolated 4-quinozolinone, and was named quinazolinone A.

291 The $[M + H]^+$ molecular ion at *m/z* 209.0932 in the ESI-HRMS spectrum resulted in a molecular
292 formula of $C_{10}H_{12}N_2O_3$ for **2** (yield 0.3 mg/L). The ^{13}C NMR spectrum presented 10 signals, which was
293 consistent with the molecular formula (Table 1). The ^1H NMR spectrum of **2** resembled that of **1** in the
294 downfield aromatic region, and the major difference is the absence of a set of signals for the additional
295 glycerol unit. Further HMBC experiment confirmed **2** is a *mono*-glycerolated 4-quinazolinone (Fig. 5).
296 Compound **2** was named quinazolinone B.

297 The 4-quinazoline alkaloids represent an important class of nitrogen-containing heterocyclic
298 compounds [26], which have highly diverse biological activities, such as antitumor, anti-inflammatory,
299 antihypertensive, antimicrobial, anticonvulsant and antifungal activities [17]. Though the basic bicyclic
300 core (the fused benzene ring and pyrimidine ring) is normally conserved in most of naturally occurring
301 4-quinazoline derivatives [26], a variety of structural substitutions have oftentimes been found on the
302 pyrimidine ring of the 4-quinazolinone. Quinazolinones A and B isolated from *Streptomyces* sp. MBT27
303 represent the first example that glycerol participates in the construction of the ring system of 4-
304 quinazolines. In this sense, quinazolinones A and B can be perceived as a new sub-branch in the family
305 of the quinazolines. Particularly, quinazolinone A contains an exciting seven-membered ring formed
306 by intermolecular etherification of two units of glycerol, and this ring is further linked with the
307 quinazolinone backbone by a spiro atom at C-2, which is unprecedented. Antimicrobial activities of
308 compounds **1** and **2** were tested against *B. subtilis* and *E. coli*. None of the compounds showed
309 antimicrobial activity against these indictor strains (data not shown). Further bioactivity screening is
310 required to find out what the biological activity of the two compounds is.
311
312 **Biosynthesis of quinazolinones A and B**
313 In our study, the production of **1** and **2** was dramatically enhanced in the cultures with 2% glycerol.
314 Elicitation by glycerol is an indication that glycerol may play a key role during their biosynthesis. The
315 aromatic ring system of quinazoline alkaloids is known to be derived from anthranilic acid, which in
316 turn is biosynthesized through the shikimate pathway [12]. In line with this, we propose that the
317 biosynthesis of the isolated quinazolinones starts from anthranilic acid, which is then converted to
318 anthranilamide (Fig. 6). Further successive attachments of two molecules of glycerol then results in
319 the formation of **2**, followed by **1**. However, multiple biosynthetic routes have been proposed for
320 quinazolinones, because the C-2 residue of the quinazoline ring may originate from various precursors.
321 For example, the C-2 and the remaining non-aromatic part of the quinazolinone alkaloid chrysogine,
322 produced by *Penicillium chrysogenum*, are biosynthesized from pyruvic acid via an NRPS system [45],

323 while the non-aromatic part of the quinazoline alkaloid peganine, produced by the plant *Peganum*
324 *harmala*, is derived from ornithine [12]. Furthermore, fumiquinazoline F originates from a fungal
325 nonribosomal peptide synthetase (TqaA) and is biosynthesized from anthranilic acid, L-tryptophan and
326 L-alanine [14].

327 In conclusion, the metabolic potential of *Streptomyces* sp. MBT27 was analyzed under different
328 nutritional conditions, showing major changes in the metabolome, depending on the carbon source
329 used. In particular, the relatively unspectacular change from 1% to 2% glycerol resulted in a surprisingly
330 global change in the secondary metabolome, with some compounds changing by almost four orders
331 of magnitude. The use of GNPS molecular networking, together with LC-MS based dereplication,
332 allowed us to annotate a cluster of quinazolinone-family molecules that connects to anthranilic acid
333 and anthranilamide. Isolation and structure elucidation revealed the novel alkaloid natural products
334 quinazolinone A and B. Based on the structures, the biosynthesis of the compounds most likely involves
335 the conversion of anthranilic acid to anthranilamide, which is subsequently attached to two glycerol
336 units, to produce compounds **1** and **2**. Identification of the biosynthetic gene cluster and subsequent
337 analysis of the individual enzymatic reactions should reveal the precise biosynthetic pathway for these
338 exciting novel molecules.

339

340 Reference list

341

342 1. Baltz RH (2008) Renaissance in antibacterial discovery from actinomycetes. Curr Opin Pharmacol
343 8:557-563

344 2. Barka EA, Vatsa P, Sanchez L, Gavaut-Vaillant N, Jacquard C, Meier-Kolthoff J, Klenk HP, Clément C,
345 Oudouch Y, van Wezel GP (2016) Taxonomy, physiology, and natural products of the
346 *Actinobacteria*. Microbiol Mol Biol Rev 80:1-43

347 3. Bentley SD, Chater KF, Cerdeno-Tarraga AM, Challis GL, Thomson NR, James KD, Harris DE, Quail MA,
348 Kieser H, Harper D, Bateman A, Brown S, Chandra G, Chen CW, Collins M, Cronin A, Fraser A,
349 Goble A, Hidalgo J, Hornsby T, Howarth S, Huang CH, Kieser T, Larke L, Murphy L, Oliver K,
350 O'Neil S, Rabbinowitsch E, Rajandream MA, Rutherford K, Rutter S, Seeger K, Saunders D,
351 Sharp S, Squares R, Squares S, Taylor K, Warren T, Wietzorrek A, Woodward J, Barrell BG,
352 Parkhill J, Hopwood DA (2002) Complete genome sequence of the model actinomycete
353 *Streptomyces coelicolor* A3(2). Nature 417:141-147

354 4. Bérdy J (2005) Bioactive microbial metabolites. J Antibiot (Tokyo) 58:1-26

355 5. Bode HB, Bethe B, Höfs R, Zeeck A (2002) Big Effects from Small Changes: Possible Ways to Explore
356 Nature's Chemical Diversity. ChemBioChem 3:619–627

357 6. Chambers MC, Maclean B, Burke R, Amodei D, Ruderman DL, Neumann S, Gatto L, Fischer B, Pratt
358 B, Egertson J, Hoff K, Kessner D, Tasman N, Shulman N, Frewen B, Baker TA, Brusniak MY,
359 Paulse C, Creasy D, Flashner L, Kani K, Moulding C, Seymour SL, Nuwaysir LM, Lefebvre B,
360 Kuhlmann F, Roark J, Rainer P, Detlev S, Hemenway T, Huhmer A, Langridge J, Connolly B,
361 Chadick T, Holly K, Eckels J, Deutsch EW, Moritz RL, Katz JE, Agus DB, MacCoss M, Tabb DL,
362 Mallick P (2012) A cross-platform toolkit for mass spectrometry and proteomics. Nat
363 Biotechnol 30:918–920

364 7. Chong J, Soufan O, Li C, Caraus I, Li S, Bourque G, Wishart DS, Xia J (2018) MetaboAnalyst 4.0: towards
365 more transparent and integrative metabolomics analysis. Nucleic Acids Res 46:W486-W494

366 8. Conti R, Chagas FO, Caraballo-Rodriguez AM, Melo WG, do Nascimento AM, Cavalcanti BC, de
367 Moraes MO, Pessoa C, Costa-Lotufo LV, Krogh R, Andricopulo AD, Lopes NP, Pupo MT (2016)
368 Endophytic Actinobacteria from the Brazilian Medicinal Plant Lychnophora ericoides Mart.
369 and the Biological Potential of Their Secondary Metabolites. Chem Biodivers 13:727–736
370 9. Cooper MA, Shlaes D (2011) Fix the antibiotics pipeline. Nature 472:32
371 10. Craney A, Ozimok C, Pimentel-Elardo SM, Capretta A, Nodwell JR (2012) Chemical perturbation of
372 secondary metabolism demonstrates important links to primary metabolism. Chem Biol
373 19:1020-1027
374 11. Cruz-Morales P, Vijgenboom E, Iruegas-Bocardo F, Girard G, Yanez-Guerra LA, Ramos-Aboites HE,
375 Pernodet JL, Anne J, van Wezel GP, Barona-Gomez F (2013) The genome sequence of
376 *Streptomyces lividans* 66 reveals a novel tRNA-dependent peptide biosynthetic system within
377 a metal-related genomic island. Genome Biol Evol 5:1165-1175
378 12. Dewick P (2009) Medicinal Natural Products: A Biosynthetic Approach. 3rd edn. ohn Wiley & Sons,
379 Chichester, UK
380 13. Du C, van Wezel GP (2018) Mining for Microbial Gems: Integrating Proteomics in the Postgenomic
381 Natural Product Discovery Pipeline. Proteomics:e1700332
382 14. Gao X, Chooi YH, Ames BD, Wang P, Walsh CT, Tang Y (2011) Fungal indole alkaloid biosynthesis:
383 genetic and biochemical investigation of the tryptoquialanine pathway in *Penicillium*
384 *aethiopicum*. J Am Chem Soc 133:2729–2741
385 15. Gaudencio SP, Pereira F (2015) Dereplication: racing to speed up the natural products discovery
386 process. Nat Prod Rep 32:779–810
387 16. Hameed A, Al-Rashida M, Uroos M, Ali SA, Arshia, Ishtiaq M, Khan KM (2018) Quinazoline and
388 quinazolinone as important medicinal scaffolds: a comparative patent review (2011-2016).
389 Expert Opin Ther Pat 28:281-297
390 17. He D, Wang M, Zhao S, Shu Y, Zeng H, Xiao C, Lu C, Liu Y (2017) Pharmaceutical prospects of
391 naturally occurring quinazolinone and its derivatives. Fitoterapia 119:136–149

392 18. Ikeda H, Ishikawa J, Hanamoto A, Shinose M, Kikuchi H, Shiba T, Sakaki Y, Hattori M, Omura S (2003)
393 Complete genome sequence and comparative analysis of the industrial microorganism
394 *Streptomyces avermitilis*. Nat Biotechnol 21:526-531
395 19. Jafari E, Khajouei MR, Hassanzadeh F, Hakimelahi GH, Khodarahmi GA (2016) Quinazolinone and
396 quinazoline derivatives: recent structures with potent antimicrobial and cytotoxic activities.
397 Res Pharm Sci 11:1-14
398 20. Kieser T, Bibb MJ, Buttner MJ, Chater KF, Hopwood DA (2000) Practical *Streptomyces* genetics. John
399 Innes Foundation, Norwich, U.K.
400 21. Kolter R, van Wezel GP (2016) Goodbye to brute force in antibiotic discovery? Nat Microbiol
401 1:15020
402 22. Kornsakulkarn J, Saepua S, Srijomthong K, Rachtawee P, Thongpanchang C (2015) Quinazolinone
403 alkaloids from actinomycete Streptomyces sp. BCC 21795. Phytochemistry Letters 12:6–8
404 23. Kshirsagar UA (2015) Recent developments in the chemistry of quinazolinone alkaloids. Org Biomol
405 Chem 13:9336-9352
406 24. Laatsch H (2012) Antibase 2012, the Natural Compound Identifier.
407 25. Martin JF, Sola-Landa A, Santos-Beneit F, Fernandez-Martinez LT, Prieto C, Rodriguez-Garcia A
408 (2011) Cross-talk of global nutritional regulators in the control of primary and secondary
409 metabolism in *Streptomyces*. Microb Biotechnol 4:165-174
410 26. Michael JP (2000) Quinoline, quinazoline and acridone alkaloids. Nat Prod Rep 17: 603–620
411 27. Nett M, Ikeda H, Moore BS (2009) Genomic basis for natural product biosynthetic diversity in the
412 actinomycetes. Nat Prod Rep 26:1362-1384
413 28. Payne DJ, Gwynn MN, Holmes DJ, Pompliano DL (2007) Drugs for bad bugs: confronting the
414 challenges of antibacterial discovery. Nat Rev Drug Discov 6:29-40
415 29. Pluskal T, Castillo S, Villar-Briones A, Orešič M (2010) MZmine 2: Modular framework for
416 processing, visualizing, and analyzing mass spectrometry-based molecular profile data. BMC
417 Bioinformatics 11:395

418 30. Rice LB (2008) Federal funding for the study of antimicrobial resistance in nosocomial pathogens:
419 no ESKAPE. J Infect Dis 197:1079-1081
420 31. Rigali S, Titgemeyer F, Barends S, Mulder S, Thomae AW, Hopwood DA, van Wezel GP (2008) Feast
421 or famine: the global regulator DasR links nutrient stress to antibiotic production by
422 *Streptomyces*. EMBO Rep 9:670-675
423 32. Romano S, Jackson SA, Patry S, Dobson ADW (2018) Extending the "One Strain Many Compounds"
424 (OSMAC) principle to marine microorganisms. Mar Drugs 16:244
425 33. Rutledge PJ, Challis GL (2015) Discovery of microbial natural products by activation of silent
426 biosynthetic gene clusters. Nat Rev Microbiol 13:509-523
427 34. Sanchez S, Chavez A, Forero A, Garcia-Huante Y, Romero A, Sanchez M, Rocha D, Sanchez B, Avalos
428 M, Guzman-Trampe S, Rodriguez-Sanoja R, Langley E, Ruiz B (2010) Carbon source regulation
429 of antibiotic production. J Antibiot (Tokyo) 63:442-459
430 35. Schulze CJ, Bray WM, Woerhmann MH, Stuart J, Lokey RS, Linington RG (2013) "Function-first" lead
431 discovery: mode of action profiling of natural product libraries using image-based screening.
432 Chem Biol 20:285–295
433 36. Shaaban KA, Shepherd MD, Ahmed TA, Nybo SE, Leggas M, Rohr J (2012) Pyramidamycins A-D and
434 3-hydroxyquinoline-2-carboxamide; cytotoxic benzamides from *Streptomyces* sp. DGC1. J
435 Antibiot (Tokyo) 65:615–622
436 37. Shannon P, Markiel A, Ozier O, Baliga NS, Wang JT, Ramage D, Amin N, Schwikowski B, Ideker T
437 (2003) Cytoscape: a software environment for integrated models of biomolecular interaction
438 networks. Genome Res 13:2498–2504
439 38. Swiatek-Polatynska MA, Bucca G, Laing E, Gubbens J, Titgemeyer F, Smith CP, Rigali S, van Wezel
440 GP (2015) Genome-wide analysis of *In vivo* binding of the master regulator DasR in
441 *Streptomyces coelicolor* identifies novel non-anonical targets. PLoS One 10:e0122479

442 39. Urem M, Swiatek-Polatynska MA, Rigali S, van Wezel GP (2016) Intertwining nutrient-sensory
443 networks and the control of antibiotic production in Streptomyces. Mol Microbiol 102:183-
444 195
445 40. van der Heul HU, Bilyk BL, McDowall KJ, Seipke RF, van Wezel GP (2018) Regulation of antibiotic
446 production in Actinobacteria: new perspectives from the post-genomic era. Nat Prod Rep
447 35:575-604
448 41. van Wezel GP, McKenzie NL, Nodwell JR (2009) Applying the Genetics of Secondary Metabolism in
449 Model Actinomycetes to the Discovery of New Antibiotics. In: Complex Enzymes in Microbial
450 Natural Product Biosynthesis, Part A: Overview Articles and Peptides. Methods in
451 Enzymology. pp 117–141. doi:https://doi.org/10.1016/s0076-6879(09)04805-8
452 42. Vater J, Crnovcic I, Semsary S, Keller U (2014) MALDI-TOF mass spectrometry, an efficient technique
453 for in situ detection and characterization of actinomycins. J Mass Spectrom 49:210–222
454 43. Wang M, Carver JJ, Phelan VV, Sanchez LM, Garg N, Peng Y, Nguyen DD, Watrous J, Kapono CA,
455 Luzzatto-Knaan T, Porto C, Bouslimani A, Melnik AV, Meehan MJ, Liu WT, Crusemann M,
456 Boudreau PD, Esquenazi E, Sandoval-Calderon M, Kersten RD, Pace LA, Quinn RA, Duncan KR,
457 Hsu CC, Floros DJ, Gavilan RG, Kleigrewe K, Northen T, Dutton RJ, Parrot D, Carlson EE, Aigle
458 B, Michelsen CF, Jelsbak L, Sohlenkamp C, Pevzner P, Edlund A, McLean J, Piel J, Murphy BT,
459 Gerwick L, Liaw CC, Yang YL, Humpf HU, Maansson M, Keyzers RA, Sims AC, Johnson AR,
460 Sidebottom AM, Sedio BE, Klitgaard A, Larson CB, Boya PC, Torres-Mendoza D, Gonzalez DJ,
461 Silva DB, Marques LM, Demarque DP, Pociute E, O'Neill EC, Briand E, Helfrich EJ, Granatosky
462 EA, Glukhov E, Ryffel F, Houson H, Mohimani H, Kharbush JJ, Zeng Y, Vorholt JA, Kurita KL,
463 Charusanti P, McPhail KL, Nielsen KF, Vuong L, Elfeki M, Traxler MF, Engene N, Koyama N,
464 Vining OB, Baric R, Silva RR, Mascuch SJ, Tomasi S, Jenkins S, Macherla V, Hoffman T, Agarwal
465 V, Williams PG, Dai J, Neupane R, Gurr J, Rodriguez AM, Lamsa A, Zhang C, Dorrestein K,
466 Duggan BM, Almaliti J, Allard PM, Phapale P, Nothias LF, Alexandrov T, Litaudon M,
467 Wolfender JL, Kyle JE, Metz TO, Peryea T, Nguyen DT, VanLeer D, Shinn P, Jadhav A, Muller R,

468 Waters KM, Shi W, Liu X, Zhang L, Knight R, Jensen PR, Palsson BO, Pogliano K, Linington RG,
469 Gutierrez M, Lopes NP, Gerwick WH, Moore BS, Dorrestein PC, Bandeira N (2016) Sharing and
470 community curation of mass spectrometry data with Global Natural Products Social
471 Molecular Networking. Nat Biotechnol 34:828-837
472 44. Winnikoff JR, Glukhov E, Watrous J, Dorrestein PC, Gerwick WH (2014) Quantitative molecular
473 networking to profile marine cyanobacterial metabolomes. J Antibiot (Tokyo) 67:105–112
474 45. Wollenberg RD, Saei W, Westphal KR, Klitgaard CS, Nielsen KL, Lysoe E, Gardiner DM, Wimmer R,
475 Sondergaard TE, Sorensen JL (2017) Chrysogine Biosynthesis Is Mediated by a Two-Module
476 Nonribosomal Peptide Synthetase. J Nat Prod 80:2131–2135
477 46. Wu C, Kim HK, van Wezel GP, Choi YH (2015) Metabolomics in the natural products field - a gateway
478 to novel antibiotics. Drug Discov Today Technol 13:11-17
479 47. Yang JY, Sanchez LM, Rath CM, Liu X, Boudreau PD, Bruns N, Glukhov E, Wodtke A, de Felicio R,
480 Fenner A, Wong WR, Linington RG, Zhang L, Debonsi HM, Gerwick WH, Dorrestein PC (2013)
481 Molecular networking as a dereplication strategy. J Nat Prod 76:1686–1699
482 48. Yoon V, Nodwell JR (2014) Activating secondary metabolism with stress and chemicals. J Ind
483 Microbiol Biotechnol 41:415-424
484 49. Zhu H, Sandiford SK, van Wezel GP (2014) Triggers and cues that activate antibiotic production by
485 actinomycetes. J Ind Microbiol Biotechnol 41:371-386
486 50. Zhu H, Swierstra J, Wu C, Girard G, Choi YH, van Wamel W, Sandiford SK, van Wezel GP (2014)
487 Eliciting antibiotics active against the ESKAPE pathogens in a collection of actinomycetes
488 isolated from mountain soils. Microbiology 160:1714–1725
489
490
491

492 **Table 1. ^{1}H and ^{13}C NMR data for compounds 1 and 2[a]**

493

NO.	1		2	
	δ_C	δ_H (mult., *J* in Hz)	δ_C	δ_H (mult., *J* in Hz)
2	79.0		73.3	
4	166.1		166.7	
4a	121.8		114.5	
5	128.8	7.88 (dd, *J* = 7.8, 1.2)	128.5	7.66 (dd, *J* = 7.8, 1.2)
6	123.0	7.07 (t, *J* = 7.8)	118.5	6.69 (td, *J* = 7.8, 1.2)
7	134.6	7.46 (td, *J* = 7.8, 1.2)	135.3	7.26 (td, *J* = 7.8, 1.2)
8	122.3	7.23 (brd, *J* = 7.8)	115.8	6.73 (brd, *J* = 7.8)
8a	143.7		148.6	
1'	73.9	4.43 (d, *J* = 9.0); 4.24 (d, *J* = 9.0)	64.5	3.67 (d, *J* = 10.8); 3.62 (d, *J* = 10.8)
2'	64.6	3.59 (d, *J* = 11.4); 3.47 (d, *J* = 11.4)	64.5	3.67 (d, *J* = 10.8); 3.62 (d, *J* = 10.8)
1''	65.7	3.86 (d, *J* = 12.6); 3.80 (d, *J* = 12.6)		
2''	102.9			
3''	61.9	3.66 (d, *J* = 3.0)		

494 [a] **1** and **2** were recorded in CD_3OD, at 298 K. All chemical shift assignments were done on the basis of

495 1D and 2D NMR techniques.

496

497 **Figure Legends**

498

499 **Fig. 1. Analysis of secondary metabolites produced by *Streptomyces* sp. MBT27.** The heat map depicts
500 the relative abundance of the metabolites (rows) produced under different growth conditions
501 (columns)

502

503 **Fig. 2. Secondary metabolite profiles found in 1% and 2% glycerol-grown cultures of *Streptomyces***
504 **sp. MBT27. a.** Thin layer chromatography of extracts from the cultures grown in MM with either 1%
505 or 2% glycerol as the carbon source. **b.** Volcano plot highlighting the differences in metabolite profiles.
506 Pink circles represent metabolites with an intensity difference of more than 4-fold (p-value ≤ 0.005)

507

508 **Fig. 3. GNPS molecular network of the ions detected in the crude extract of *Streptomyces* sp. MBT27.**
509 Cultured were grown in MM with 2% glycerol, with an enlargement of the clusters including the
510 dereplicated and identified metabolites. Green nodes represent the dereplicated metabolites, while
511 blue nodes represent the masses upregulated when glycerol concentration was increased from 1% to
512 2%

513 **Fig. 4. Chemical structures of quinazolinones A (1) and B (2).**

514

515 **Fig 5. Key COSY ( ) and HMBC ( ) correlations for 1 and 2.**

516

517 **Fig. 6 Proposed biosynthetic pathway for quinazolinone A (1) and B (2).**

518

519

520 **Fig. 1.**

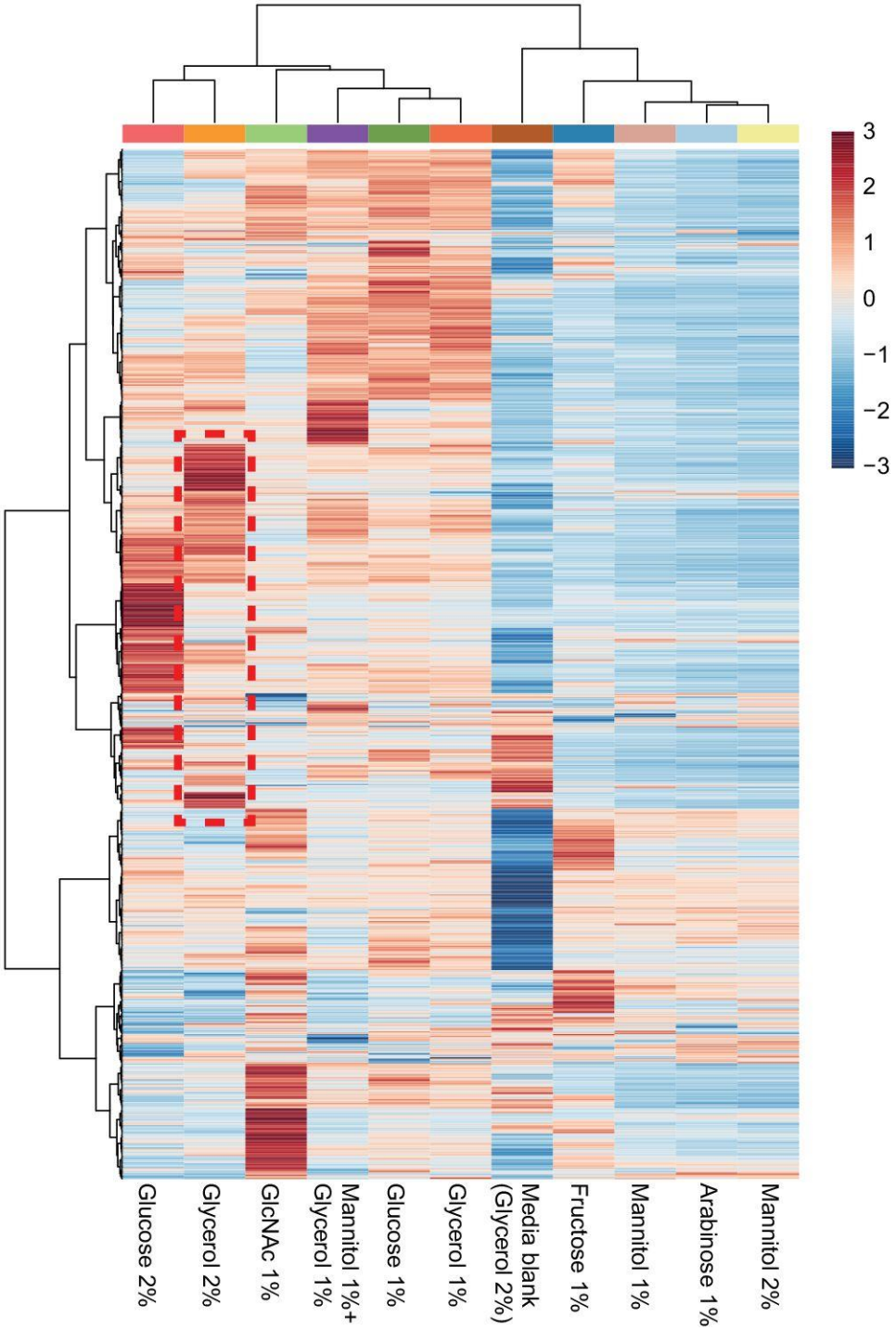

521

522

523 **Fig. 2.**

524

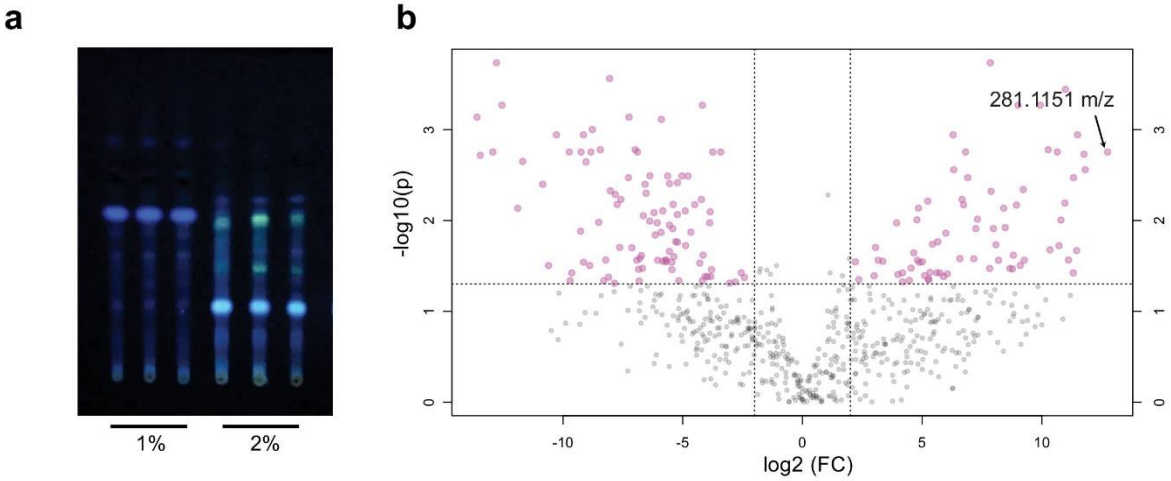

525

526

527 **Fig. 3.**

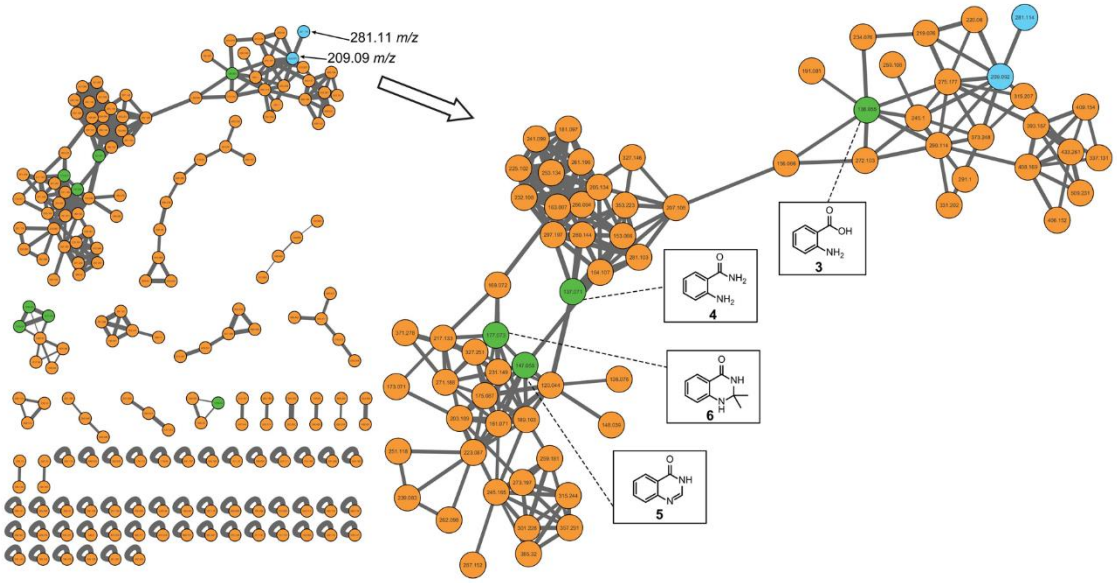

528

Fig. 4

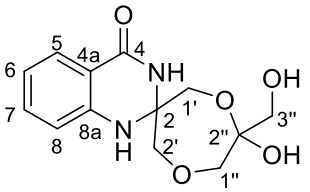

Quinazolinone A (**1**)

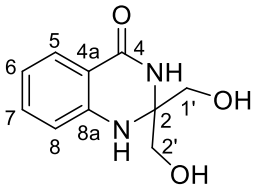

Quinazolinone B (**2**)

Fig. 5

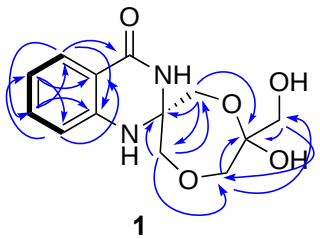

1

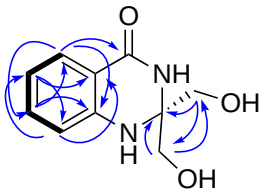

2
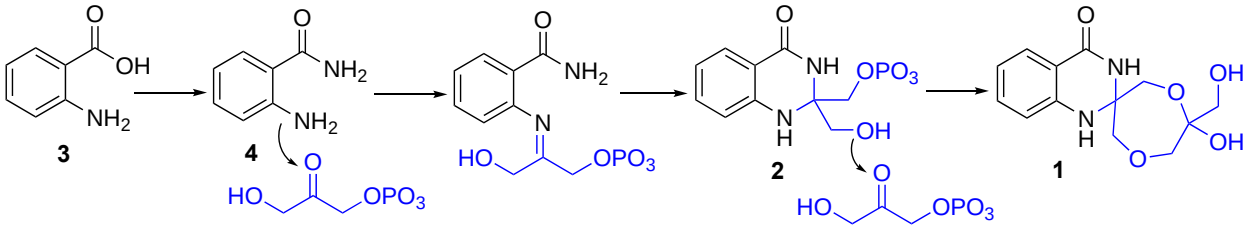
Fig. 6